PHYSICAL REVIEW E **78**, 025205(R) (2008)

Scenarios for generalized synchronization with chaotic driving

Thounaojam Umeshkanta Singh, Amitabha Nandi, and Ramakrishna Ramaswamy
School of Physical Sciences, Jawaharlal Nehru University, New Delhi 110 067, India
(Received 21 April 2008; published 26 August 2008)

In chaotically driven nonlinear dynamical systems, weak generalized synchrony can arise through distinct scenarios or routes in a manner similar to the onset of low-dimensional chaos or the creation of strange nonchaotic attractors in quasiperiodically driven systems. The limit sets of the dynamics for weak generalized synchronization are nonchaotic—the Lyapunov exponent is nonpositive—and are geometrically strange. Quantitative measures related to the parameter sensitivity exponent and finite-time Lyapunov exponent distributions can be defined in order to characterize generalized synchronization.

DOI: 10.1103/PhysRevE.78.025205 PACS number(s): 05.45.Xt

The resurgence of interest in the synchronization of nonlinear dynamical systems in recent years has given the insight that there can be several different forms of synchrony in coupled systems [1]. Depending on the form of the coupling—whether uni- or bidirectional—and on the nature of the dynamics, there can be complete [2], lag [3], or phase [4] synchronization, while in extended dynamical systems [5], or when there is time delay, other forms of synchrony are known [6].

When one nonlinear dynamical system is unidirectionally modulated by another, *generalized* synchronization (GS) can result [7,8] if the driving is of appropriate strength. Given a drive with dynamics

$$\dot{\mathbf{u}} = F(\mathbf{u}) \tag{1}$$

and response system

$$\dot{\mathbf{x}} = G(\mathbf{x}, \mathbf{u}), \tag{2}$$

GS implies the existence of a unique functional dependence $\mathbf{x}=\mathbf{\Phi}[\mathbf{u}]$ [7] when the vectors fields of the drive and response, F and G, are continuous and differentiable. Regimes of GS are defined as either strong or weak depending on whether Φ is differentiable or not [9,10]. The presence of GS can be determined, for example, by constructing copies of the response system

$$\dot{\mathbf{x}}' = G(\mathbf{x}', \mathbf{u}) \tag{3}$$

and examining the complete synchronization between $\mathbf{x}$ and $\mathbf{x}'$ [11].

Extensive studies of systems such as Eqs. (1) and (2) in the past decades, particularly for chaotic dynamics in $\mathbf{u}$ in the so-called "master-slave" scenario [2], have established that complete synchronization occurs when subsystem Lyapunov exponents (in effect, those characteristic of the slave system) are all nonpositive. Similarly, nonautonomous systems with periodic, quasiperiodic, or stochastic driving have been studied in the context of synchronization as well, and the manner in which systems subject to a common noise show synchronization has been addressed in a number of studies [12,13]. Nevertheless, an understanding of how synchronization comes about in such general settings is still incomplete.

In this work, we show that GS can occur via distinct bifurcation routes. Such scenarios have been described earlier for the onset of low-dimensional chaos [14], and we find that the different scenarios through which weak GS occurs in chaotically driven dynamical systems have parallels in the routes by which strange nonchaotic attractors can be formed in quasiperiodically driven systems. These include analogs of the blowout, doubling, and saddle-node bifurcations, as well as fractalization. Our results are illustrated below for driven mappings for simplicity, although we have verified that similar behavior occurs in continuous-time dynamical systems as well [15].

As a model for the response, we first consider a dynamical system introduced by Grebogi *et al.* [17]:

$$x_{n+1} = 2r \tanh x_n \cos 2\pi u_n, \tag{4}$$

where $x \in \mathbb{R}$ and $r>0$, and u is the drive. The chaotic drive that we employ is provided by the series $\{u\}$ in the generalized baker map [16],

$$u_{n+1} = \begin{cases} bu_n, & v_n < a, \\ b + (1-b)u_n, & v_n \geqslant a, \end{cases} \tag{5a}$$

$$v_{n+1} = \begin{cases} v_n/a, & v_n < a, \\ (v_n - a)/(1-a), & v_n \geqslant a, \end{cases} \tag{5b}$$

with $a=b=0.45$.

When the map, Eq. (4), is subject to a quasiperiodic drive, for example, through the irrational rigid rotation

$$u_{n+1} = u_n + \omega \bmod 1, \tag{6}$$

with ω chosen to be an irrational number [such as the inverse golden mean ratio $\omega=(\sqrt{5}-1)/2$], it has been shown that the resulting attractor is both strange and nonchaotic above $r=1$ [17,18]. The dynamics that obtains from the chaotic baker drive for a typical set of initial conditions is shown in Fig. 1. This orbit is also stable, in the sense that two copies of the response driven by a common chaotic drive will show perfect synchrony [11]. The subsystem Lyapunov exponent is negative, and it may be possible to show, using arguments that parallel the quasiperiodic case [17], that the limit set in Fig. 1(b) is strange and nonchaotic. By changing the initial conditions on the drive, the dynamics of the response is altered, although qualitatively it remains similar. Since the functional dependence of x on u is nonsmooth—i.e., nondif-

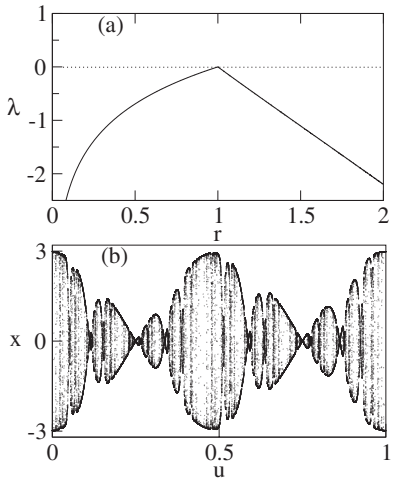

FIG. 1. (a) The subsystem Lyapunov exponent for Eq. (4) driven by the chaotic baker map, Eq. (5a), computed from an ensemble of random initial x_0 as a function of the parameter r; there is a blowout bifurcation $r=1$. (b) Limit set for $r=1.5$ on which the dynamics are both aperiodic and nonchaotic.

ferentiable—as shown by the graph in Fig. 1(b), a regime of weak GS is manifested [9,10].

The similarity with the strange nonchaotic dynamics created by quasiperiodic driving [19] is both qualitative and quantitative, and this can be seen by considering the driven logistic mapping

$$x_{n+1} = \alpha x_n(1 - x_n)(1 + \varepsilon \cos 2\pi u_n), \tag{7}$$

where a number of other scenarios are known for the creation of strange nonchaotic attractors (SNAs) when u is quasiperiodic. These are the so-called fractalization [20], torus collision [21], and intermittency routes [22] that have their origin in crises and period-doubling and saddle-node bifurcation routes to chaos in unforced systems. The dynamical phase diagram for the chaotically forced logistic mapping is shown in Fig. 2, and the gross similarity to the dynamical states

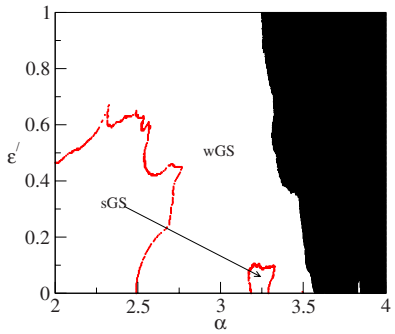

FIG. 2. (Color online) Schematic phase diagram for the logistic map driven by the chaotic baker map, Eq. (5a), as a function of α and rescaled parameter $\varepsilon' = \varepsilon/(4/\alpha - 1)$. In the chaotic (black) regions there is no synchronization, while there is GS in the nonchaotic regions (white). Regions of weak GS (wGS) and strong GS (sGS) are separated by the red (gray) curve. Note a small window of nonchaotic behavior corresponding to the period-3 orbit inside the chaotic region.

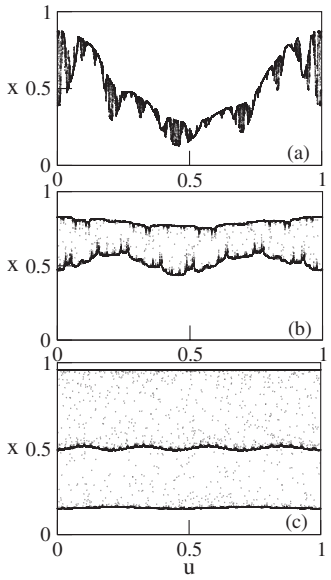

FIG. 3. Typical limit sets for nonsmooth or weak GS in the driven logistic map, showing (a) fractalization ($\alpha=2.3$, $\varepsilon'=0.7$) with $\lambda=-0.572$, (b) doubling collisions ($\alpha=3.2$, $\varepsilon'=0.15$) with $\lambda=-0.531$ when there is the collision of the stable doubled graph with its unstable parent, and (c) intermittency due to an interior crisis inside the period-3 window ($\alpha=3.832$, $\varepsilon'=0.03$) with $\lambda=-0.264$.

obtained via quasiperiodic driving is evident [22]. The entire region of nonchaotic dynamics (the white region in Fig. 2) exhibits generalized synchrony, and this can be further divided into weak and strong GS regions. The boundary separating the two regimes is estimated from the Lyapunov dimension [9].

A systematic exploration of the parameter space shows that there are parallels between the transition to weak GS and the creation of SNAs in the corresponding quasiperiodically driven system. We briefly describe these below, highlighting the similarities as well as the differences.

Fractalization. In this scenario, the single-valued graph $x(u)$ gradually wrinkles to become nonsmooth, as can be judged by, say, the Hölder exponent [10]. Like the case of quasiperiodic fractalization [20], there is no abrupt transition as at a bifurcation. However, strong GS transforms to weak GS; see Fig. 3(a).

Doubling collisions. For sufficiently small values of the parameters α or ε', the graph $x(u)$ is single valued and smooth. As the parameters are increased, there is period doubling and the graph $x(u)$ becomes double valued. With increasing parameter, the two branches of the graph wrinkle and eventually collide, forming a nonsmooth graph. The conditional Lyapunov exponent remains negative, and hence this is a case of weak GS. In the quasiperiodic case, the collision of the two branches of the doubled orbit occurs simultaneously with their collision with the unstable parent orbit [21], whereas this is not the case here; see Fig. 3(b).

Intermittency. In the intermittency scenario, a saddle-node bifurcation leads to an intermittent dynamical state [22] in which the subsystem Lyapunov exponent is negative. The graph $x(u)$ is multivalued and nondifferentiable; see Fig. 3(c).

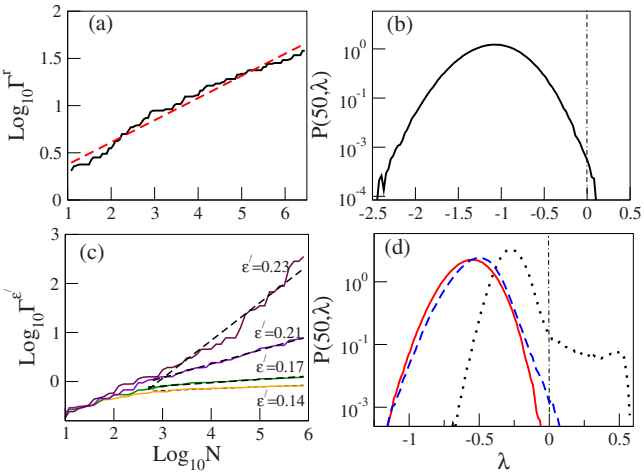

FIG. 4. (Color online) Measures to quantify the dynamics of wGS in the chaotically driven mappings, Eq. (4) in (a) and (b) and Eq. (7) in (c) and (d). (a) Parameter sensitivity of a typical limit set in Eq. (8) with $r=1.5$ showing power-law dependence with sensitivity exponent $\mu \approx 0.24$. (b) The probability distribution of finite-time Lyapunov exponents (FTLEs) at this parameter value is Gaussian. (c) Sensitivity exponent for the logistic map along $\alpha=3.3$ for different ε'. At $\varepsilon'=0.14$, $\mu \approx 0.04$; $\varepsilon'=0.17$, $\mu \approx 0.07$; $\varepsilon'=0.21$, $\mu \approx 0.28$; and $\varepsilon'=0.23$, $\mu \approx 0.77$. (d) Probability distribution of FTLEs for orbit segments of length $N=50$ for the three different scenarios shown in Fig. 3: fractalization (solid line), doubling (dashed line), and intermittency (dotted line).

In all the cases of weak GS above, different trajectories on the graph $x(u)$ will converge and eventually coincide as long as they are started with the same initial conditions *in the drive* u. The dependence on the chaotic drive can be quantified via measures akin to the phase sensitivity [23] and parameter sensitivity [20] exponents that have been introduced earlier in the study of SNAs. In the present instance, the sensitivity with respect to a system parameter (denoted here by β)

$$\Gamma_N = \min_{x_0,u_0} \left\{ \max_{1<k<N} \left| \frac{dx_k}{d\beta} \right| \right\} \tag{8}$$

proves to be more appropriate to use for characterization of the limit sets. When the underlying structure is strange, this quantity scales as a power law in the length of the orbit [20]—namely, $\Gamma_N \simeq N^{\mu}$.

Figure 4(a) shows the parameter sensitivity, with exponent $\mu \approx 0.24$, for a limit set in the map, Eq. (4), at $r=1.5$. Similar results for the driven logistic map, Eq. (7), in the weak GS region along the line $\alpha=3.3$ for different ε' values are shown in Fig. 4(c). When there is strong GS, the growth of parameter sensitivity saturates and the exponent is zero; a nonzero value for μ indicates weak GS.

Additional characterization is provided by the distribution of finite-time Lyapunov exponents that probe the local structure of the regions covered by the orbit in the phase space. While the subsystem Lyapunov exponent (namely, that corresponding to the x dynamics) is indeed negative, over finite time intervals the local Lyapunov exponent can be positive, as on SNAs [23]. The distribution of finite-time Lyapunov exponents (FTLEs) [24], $P(N,\lambda)$, is the probability that the Lyapunov exponent in a time interval N lies in $[\lambda, \lambda+d\lambda]$. When there is GS, the mean of this distribution is negative as can be seen in Figs. 4(b)–4(d) and the distribution is essentially normal for the cases of weak GS formed via the blowout (solid line), fractalized (solid line), and doubling (dashed line) routes, in contrast to the analogous SNAs where there is a characteristic exponential tail [23]. This is a consequence of the chaotic drive: correlations die out rapidly and the FTLEs satisfy the central-limit theorem [25]. In the intermittency route (dotted line), as in all instances of intermittent dynamics [26], there is an exponential tail that extends into the positive-λ region; see Fig. 4(d).

The above measures provide a quantitative characterization of the weak GS state and should prove useful in the analysis of experiments [27] where GS occurs. As has been pointed out, GS is particularly important when considering an interacting ensemble of dynamical systems that are nonidentical, as frequently arises in natural situations. Examples can be drawn from numerous areas—physiological processes [28], neuronal systems [29], ecological systems [30], and financial markets [31], for instance. The emergence of synchrony in such cases is both ubiquitous and unexpected, since distinct dynamical systems would in general have very different internal time scales.

Our main result in this work is that there are distinct routes to weak GS—namely, characteristic mechanistic scenarios via which such motion is created. The limit sets of the response dynamics, which are unique (if possibly multivalued) functions of the drive, bear a strong qualitative and quantitative resemblance to corresponding attractors when the motion is strange and nonchaotic. Indeed, strange nonchaotic motion, which is observed in quasiperiodically driven systems, should be properly viewed as a manifestation of weak or nonsmooth GS. The present results also suggest, by implication, that it may be possible to characterize the state of generalized synchrony in a more definitive manner—say, by a suitable extension of the results of Sturman and Stark [32].

We have verified the above observations in other maps and flows, and with a variety of chaotic drives. Depending on the nature of the drive dynamics [33], though, the regime of strong GS may not exist: all GS is weak. A complete discussion of the different transitions from regimes of GS to unsynchronized dynamics will be presented elsewhere [15].

The creation of stable aperiodic behavior has been a major objective in the study of driven dynamical systems both from the point of view of applications [34] and as a means of understanding the manner in which natural systems maintain stability and rhythms in spite of their intrinsic stochasticity [28,35,36]. Generalized synchronization is a robust process, and the existence of definitive mechanisms through which this objective can be achieved suggests that it can be engineered and controlled in practical applications.

We thank Awadhesh Prasad for discussions and comments on the manuscript and the CSIR, India for support of T.U.S.

[1] A. Pikovsky, M. Rosenblum, and J. Kurths, *Synchronization: A Universal Concept in Nonlinear Sciences* (Cambridge University Press, Cambridge, England, 2001).
[2] L. M. Pecora and T. L. Carroll, Phys. Rev. Lett. **64**, 821 (1990).
[3] M. G. Rosenblum, A. S. Pikovsky, and J. Kurths, Phys. Rev. Lett. **78**, 4193 (1997).
[4] M. G. Rosenblum, A. S. Pikovsky, and J. Kurths, Phys. Rev. Lett. **76**, 1804 (1996).
[5] S. Boccaletti, J. Bragard, F. T. Arecchi, and H. Mancini, Phys. Rev. Lett. **83**, 536 (1999).
[6] H. U. Voss, Phys. Rev. Lett. **87**, 014102 (2001).
[7] N. F. Rulkov, M. M. Sushchik, L. S. Tsimring, and H. D. I. Abarbanel, Phys. Rev. E **51**, 980 (1995).
[8] L. Kocarev and U. Parlitz, Phys. Rev. Lett. **76**, 1816 (1996).
[9] K. Pyragas, Phys. Rev. E **54**, R4508 (1996).
[10] B. R. Hunt, E. Ott, and J. A. Yorke, Phys. Rev. E **55**, 4029 (1997).
[11] H. D. I. Abarbanel, N. F. Rulkov, and M. M. Sushchik, Phys. Rev. E **53**, 4528 (1996).
[12] A. Maritan and J. R. Banavar, Phys. Rev. Lett. **72**, 1451 (1994).
[13] C. Zhou and J. Kurths, Phys. Rev. Lett. **88**, 230602 (2002).
[14] J. P. Eckmann and D. Ruelle, Rev. Mod. Phys. **57**, 617 (1985).
[15] T. U. Singh and R. Ramaswamy (unpublished).
[16] J. D. Farmer, E. Ott, and J. A. Yorke, Physica D **7**, 153 (1983).
[17] C. Grebogi, E. Ott, S. Pelikan, and J. Yorke, Physica D **13**, 261 (1984).
[18] G. Keller, Fundam. Math. **151**, 139 (1996).
[19] A. Prasad, S. S. Negi, and R. Ramaswamy, Int. J. Bifurcation Chaos Appl. Sci. Eng. **11**, 291 (2001).
[20] T. Nishikawa and K. Kaneko, Phys. Rev. E **54**, 6114 (1996).
[21] J. F. Heagy and S. M. Hammel, Physica D **70**, 140 (1994).
[22] A. Prasad, V. Mehra, and R. Ramaswamy, Phys. Rev. Lett. **79**, 4127 (1997).
[23] A. S. Pikovsky and U. Feudel, Chaos **5**, 253 (1995).
[24] H. D. I. Abarbanel, R. Brown, and M. B. Kennel, J. Nonlinear Sci. **2**, 343 (1991).
[25] A. Prasad and R. Ramaswamy, Phys. Rev. E **60**, 2761 (1999).
[26] S. Datta and R. Ramaswamy, J. Stat. Phys. **113**, 283 (2003).
[27] A. Kittel, J. Parisi, and K. Pyragas, Physica D **112**, 459 (1998); A. Uchida, R. McAllister, R. Meucci, and R. Roy, Phys. Rev. Lett. **91**, 174101 (2003), D. Y. Tang, R. Dykstra, M. W. Hamilton, and N. R. Heckenberg, Phys. Rev. E **57**, 5247 (1998).
[28] L. Glass, Nature (London) **410**, 277 (2001).
[29] S. J. Schiff, P. So, T. Chang, R. E. Burke, and T. Sauer, Phys. Rev. E **54**, 6708 (1996).
[30] B. Blasius, A. Huppert, and L. Stone, Nature (London) **399**, 6734 (1999).
[31] J. P. Loy and C. R. Weiss, Econ. Lett. **85**, 123 (2004).
[32] J. Stark, Physica D **109**, 163 (1997); R. Sturman and J. Stark, Nonlinearity **13**, 113 (2000).
[33] Using the Ulam map $u_{n+1}=4u_n(1-u_n)$ or the variable v_n in the baker map as the drive does not give any regime of smooth or strong GS.
[34] C. S. Zhou and T. L. Chen, Europhys. Lett. **38**, 261 (1997).
[35] A. J. Mandell and K. A. Selz, J. Stat. Phys. **70**, 355 (1993).
[36] M. Kaern *et al.*, Nat. Rev. Genet. **6**, 451 (2005).